Sb surfactant mediated growth of InAs/AlAs0.56Sb0.44 strained quantum well for intersubband absorption at 1.55 μm

Yu Zhao, Julien Nicolaï, Nicolas Bertru, Hervé Folliot, Mathieu Perrin, Christophe Gatel, Bénédicte Warot-Fonrose, Anne Ponchet

Sb surfactant mediated growth of InAs/AlAs$_{0.56}$Sb$_{0.44}$ strained quantum well for intersubband absorption at 1.55 μm

Yu Zhao, Julien Nicolaï, Nicolas Bertru, Hervé Folliot, Mathieu Perrin, Christophe Gatel, B. Warot-Fonrose, and Anne Ponchet

Citation: Appl. Phys. Lett. **106**, 081908 (2015); doi: 10.1063/1.4913845
View online: https://doi.org/10.1063/1.4913845
View Table of Contents: http://aip.scitation.org/toc/apl/106/8
Published by the American Institute of Physics

Sb surfactant mediated growth of InAs/AlAs$_{0.56}$Sb$_{0.44}$ strained quantum well for intersubband absorption at 1.55 μm

Yu Zhao,[1] Julien Nicolaï,[2] Nicolas Bertru,[1] Hervé Folliot,[1] Mathieu Perrin,[1] Christophe Gatel,[2] B. Warot-Fonrose,[2] and Anne Ponchet[2]
[1]*Université Européenne de Bretagne, INSA, FOTON, UMR-CNRS 6082, 20 Avenue des Buttes de Coësmes, 35708 Rennes, France*
[2]*CEMES CNRS-UPR8011, Université de Toulouse, 31055 Toulouse, France*

(Received 28 November 2014; accepted 18 February 2015; published online 25 February 2015)

Surfactant mediated growth of strained InAs/AlAs$_{0.56}$Sb$_{0.44}$ quantum wells on InP (001) substrate is investigated. X ray diffraction and transmission electron microscopy analysis reveal that the supply of antimony on InAs surface delays the 2D to 3D growth transition and allows the growth of thick InAs/AlAsSb quantum wells. Quantum well as thick as 7 ML, without defect was achieved by Sb surfactant mediated growth. Further high resolution transmission electron microscopy measurement and geometric phase analysis show that InAs/AlAsSb interfaces are not abrupt. At InAs on AlAsSb interface, the formation of a layer presenting lattice parameter lower than InP leads to a tensile stress. From energetic consideration, the formation of As rich AlAsSb layer at interface is deduced. At AlAsSb on InAs interface, a compressive layer is formed. The impact on optical properties and the chemical composition of this layer are discussed from microscopic analysis and photoluminescence experiments. © *2015 AIP Publishing LLC*.
[http://dx.doi.org/10.1063/1.4913845]

Inter-Subband Transitions (ISBT) involve only one type of carriers, generally in the conduction band. Due to their ultra-fast dynamics and large non-linearity,[1,2] ISBT based devices are excellent candidates for the development of optoelectronics devices working at data rates exceeding 100 Gbps.[3,4] To achieve ISBT operating in the 1.55 μm telecom band, a huge conduction band offset is necessary and only a limited number of material combinations such as GaN/AlGaN,[5] (CdS/ZnSe)/BeTe,[6] and InGaAs/AlAsSb[7] meets this requirement. The latter material combination can be lattice matched to InP, making it fully compatible with the standard telecom device technology, and thus very promising for ultrafast telecom applications. However, growth of InGaAs/AlAsSb Quantum Wells (QWs) is still quite challenging. Number of elements is changed at interfaces and both Sb and In elements show large segregation to the growth front. It results in the formation of graded interfaces which shift ISBT at wavelengths longer than 1.55 μm.[8,9] The insertion of AlAs thin layers at interfaces which limits inter-diffusion[10] and (/or) the use of InGaAs alloys with high In content[11] to increase the quantum confinement have been proposed to blue shift the ISBT. Despite these procedures, ISBT observation at 1.55 μm in single QW has been not yet reported in this material system.

The growth of pure InAs/AlAsSb QWs would allow a larger conduction band offset than in InGaAs/AlAsSb QWs, which is favorable for ISBT at 1.55 μm. Moreover, reducing the number of atomic species switched at interfaces simplifies interface growth. However, the 3.2% mismatch between InAs and InP lattice parameters leads to a transition from a two dimensional (2D) to a three dimensional (3D) growth mode between 2 and 3 ML.[12,13] We have shown that Sb surfactant mediated growth prevents InAs 3D growth up to 14 ML on Ga$_{0.47}$In$_{0.53}$As matrix.[14] In order to achieve InAs/AlAsSb QWs, we propose to use Sb-mediated growth of InAs on AlAs$_{0.56}$Sb$_{0.44}$ lattice matched to InP. Structural properties of thick InAs deposits were analyzed by X-Ray Diffraction (XRD) and High Resolution Transmission Electron Microscopy (HREM). Optical properties of InAs/AlAsSb QWs were examined using Photoluminescence (PL) and the results are discussed in relation with microscopic analysis.

All the samples were grown by solid source molecular beam epitaxy on InP (001) substrates with a Riber compact 21 system. During the whole growth runs, the substrate temperature was set at 450 °C resulting from a compromise between AlAsSb and InAs optimum growth temperatures. The substrate temperature was monitored with an optical pyrometer, calibrated from InP oxide layer desorption temperature. The beam equivalent pressure ratio between group V and III elements was kept near unity to control the Sb and As incorporation in AlAs$_{0.56}$Sb$_{0.44}$ alloy. After oxide desorption and InP buffer layer deposition, a 15 nm AlAsSb layer was grown and InAs layers of various thicknesses were deposited. The InAs growth rate was set at 0.3 ML/s, and the Sb beam equivalent pressure supplied on InAs surface was maintained at 3.4×10^{-7} Torr. Growth interruptions under mixed As and Sb fluxes of 5 s and 30 s, respectively, were performed before and after the InAs deposit. Then a 15 nm AlAs$_{0.56}$Sb$_{0.44}$ layer was grown. Finally, a 5 nm lattice matched GaAsSb layer was deposited on top of the structure to prevent oxidation. High-resolution XRD patterns were measured on a Bruker AXS D8 system. A double-Ge (220)-crystal monochromator was employed. Transmission Electron Microscopy (TEM) observations were made on cross-sectional lamellas thinned in the [1-10] direction by mechanical polishing and ion milling. Dark-field images were recorded on a Philips CM20 system at an accelerating voltage of 200 kV. HREM observations were performed at

200 kV on a TECNAI F-20 microscope equipped with a spherical aberration corrector, which allows to avoid the delocalization effect at interfaces and to achieve a 0.12 nm spatial resolution. PL measurements were carried out at 15 K in a closed cycle cryostat. A 532 nm laser was used as an excitation source.

Single InAs QWs with thicknesses from 5 to 13 ML were achieved under Sb mediated growth procedure. XRD patterns performed at the vicinity of InP(004) reflection are reported in Figure 1. In absence of periodic structures, the XRD patterns are the results of interference between waves scattered in the substrate, barriers, and cap layers. The intensity modulation (Pendellösung fringes) is related to the layer flatness and stress relaxation.[15,16] At the beginning of the stress relaxation, the Pendellösung fringes fade away and the radiation background due to incoherent scattering drastically increase. In Figure 1, Pendellösung fringes are obviously detected up to 7 ML. Thus, the critical thickness is estimated to be higher than 7 ML. Note that during the InAs growth, a critical thickness for 2D-3D transition between 2 and 3 ML has been reported for similar growth conditions but without Sb supplied on surface.[12,13]

Figure 2 shows dark-field TEM cross-sectional images from 7 ML to 12 ML InAs QWs. For the first QW (Figure 2(a)), no extended defect was observed over a large area. Interfaces are flat and the thickness of InAs layer is homogeneous, showing that a 2D growth mode with a full elastic accommodation of the misfit is achieved. For the 12 ML QW (Figure 2(b)), relatively flat interfaces are also observed, showing that even for large deposit, the 3D growth mode is delayed by the supply of Sb on surface. However, several dark lines are observed over the InAs layer. They are identified as signatures of mixed-type 60° dislocations indicating that plastic strain relaxation has occurred for the 12 ML InAs sample.

7 ML-thick InAs QW assuming a square composition profile, present from tight-binding calculations,[17] an ISBT around 1.55 μm. However, intermixing and segregation lead to a shift of ISBT to longer wavelength.[10] In order to investigate the actual profile of surfactant mediated grown InAs QW, a strain analysis was performed at a very local scale applying the Geometric Phase Analysis (GPA) to an HREM

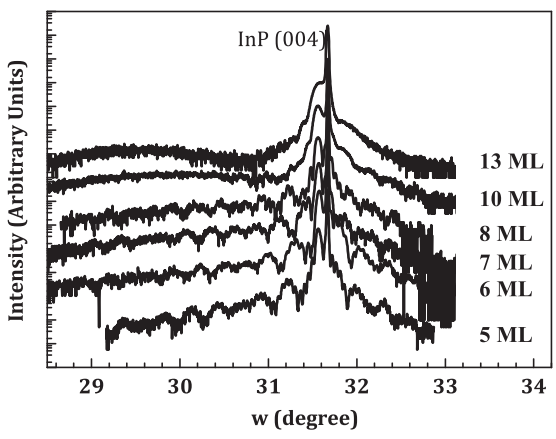

FIG. 1. ω-2θ scans XRD pattern of 5 to 13 ML thick InAs QW in AlAsSb matrix near the (004) InP reflection.

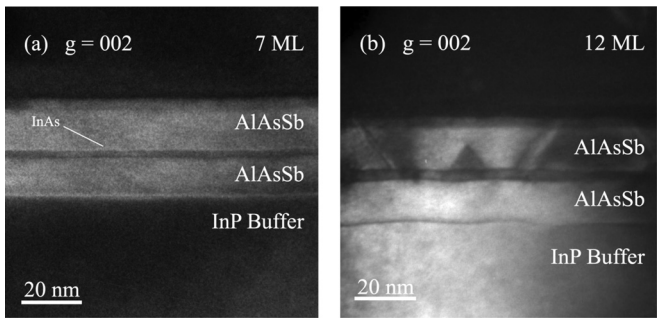

FIG. 2. Transmission electron microscopy dark-field images from 7 ML (a) and 12 ML (b) InAs/AlAsSb QW samples.

image (Figure 3(a)). The GPA method captures the variations with respect to a reference zone of the in-plane and out-of-plane lattice parameters, ε_{xx} and ε_{yy}, respectively.[18]

The reference zone was taken in the first $AlAs_{0.56}Sb_{0.44}$ barrier, sufficiently far from the QW to avoid interfacial gradient, and in the following will be considered unstrained. The mapping of ε_{xx}, the variation of the in-plane lattice parameter, is homogeneous (not shown), indicating a full elastic accommodation of the lattice mismatch. The mapping of ε_{yy}, the variation of the out-of-plane lattice parameter, is reported in Fig. 3(b) and its profile along the growth axis [001], averaged over 15 nm in the in-plane direction [110] is reported in Fig. 3(c). For a material under tetragonal strain, ε_{yy} is related to the misfit (f) and to the physical out-of-plane internal strain $\varepsilon^{\perp}_{phys}$ by

$$\varepsilon_{yy} = f + \varepsilon^{\perp}_{phys} = f\left[1 + 2\frac{C_{12}}{C_{11}}\right], \quad (1)$$

where C_{11} and C_{12} are the elastic coefficients (83.3 GPa and 45.3 GPa, respectively, for InAs).[19]

Having a lattice misfit of 3.2% with InP, a coherently strained InAs layer is expected to produce an ε_{yy} of 6.7%. This value must be minored by surface relaxation due to thinning and the shouldering at $\varepsilon_{xx} = 5\%$ in the region from 3 nm to 4 nm in Figure 3(c) can thus be attributed to InAs. Besides that, other features are observed in the ε_{yy} profile. First at InAs on AlAsSb interface, a large negative ε_{yy} peak indicates that this interface is under tensile stress. The possible ternary alloys presenting a negative misfit are "As-rich" $AlAs_ySb_{1-y}$ ($y > 0.56$) and "Al-rich" $Al_xIn_{1-x}As$ ($x > 0.48$) and more generally AlAs rich (with misfit f of -3.6%, C_{11} and C_{12} of 118 and 53 GPa,[19] respectively, pure AlAs coherent to InP substrate would have an out-of-plane strain of -3.0%, which corresponds to an ε_{yy} of -6.6%). Since Al for In exchange at this interface is very unlikely due to the stronger AlAs chemical bond in comparison with InAs, the formation of $Al_xIn_{1-x}As$ can be reasonably excluded.[20] In contrast, antimonide chemical bonds are weaker than arsenide ones and Sb is well known to be displaced by As at interface and to segregate to the surface.[21–23] These effects produce a depletion of Sb in the upper atomic layers of the barriers, i.e., "As rich" $AlAs_ySb_{1-y}$. To summarize, the formation of AlAs-rich layer at InAs on AlAsSb interface is deduced from experimental strain profile.

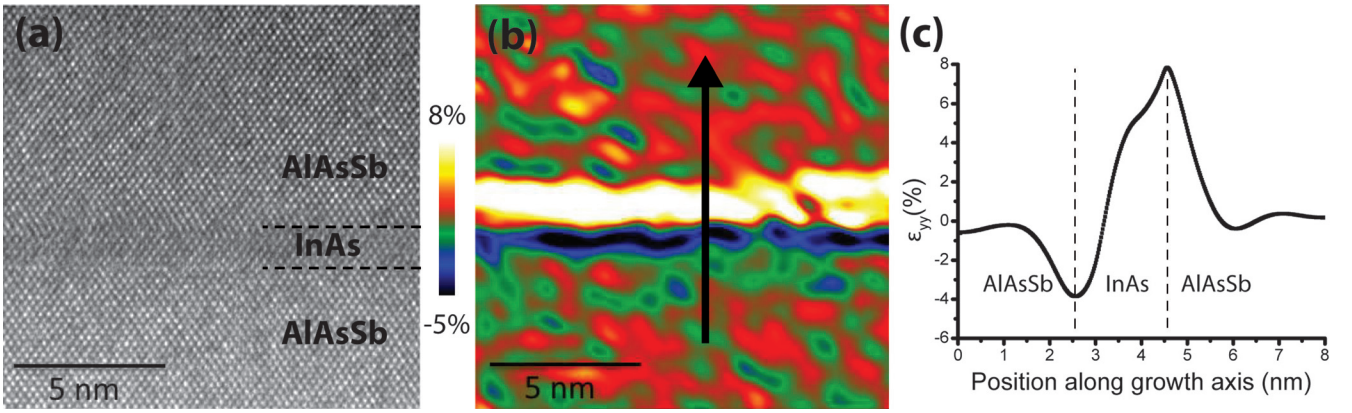

FIG. 3. (a) HREM image in $[1\bar{1}0]$ zone axis of the 7 ML thick InAs QW. (b) Map of the out-of-plane variations of the lattice parameter ε_{yy} determined from the geometric phase analysis (0.8 nm spatial resolution). (c) ε_{yy} profile along the growth direction. The arrow indicates the growth direction.

At AlAsSb on InAs interface region, an opposite behavior with an out-of-plane strain significantly larger than expected for pure InAs is observed. In other words, a layer with a lattice constant larger than InAs is formed. Alloys leading to this large compressive stress can be formed by incorporation in the upper barrier of Indium or (and) Antimony. Both elements are well known to segregate to the growth front and induced graded profile at interface.[24]

In Figure 4(a), it is reported PL peak intensity and linewidth measured at 20 K from samples with various QW thickness from 5 to 10 ML. From 5 to 7 ML thick QWs, the PL intensity increases and then drastically decreases. This trend is related to plastic relaxation onset for thick QWs. A critical thickness comparable with one deduced from XRD is obtained. PL linewidths around 60 meV are measured. Such large linewidths are due to the small QW thickness and the huge electron confinement in QWs, which enhances effect of QW thickness fluctuation. From PL energy vs thickness curves reported in Fig. 4(b), a QW thickness fluctuation around 1 ML InAs is deduced, in agreement with flat interfaces observed by TEM.

The theoretical interband transition energies for InAs/AlAsSb QWs with ideally abrupt interfaces are shown (black line) in Fig. 4(b). Calculations were done using a 6 band k·p code with material parameters from Ref. 25, assuming a conduction band offset of 1.8 eV. The strain effect on band structure is taken into account. Experimental PL energies are lower than calculated ones for every nominal thickness. The formation of unintentional layers at interfaces revealed by TEM could be the origin of such discrepancies. In order to estimate changes induced by interfacial layers, complementary k·p calculations, assuming various interfaces were performed. In these calculations, indium desorption is considered negligible at the growth temperature used. The amount of Indium inside the whole structure is thus assumed to be constant. In other words, if indium segregates from InAs QW to AlAsSb barriers, in accordance QW thickness is reduced. In contrast, for antimony we consider desorption and, its amount can vary.

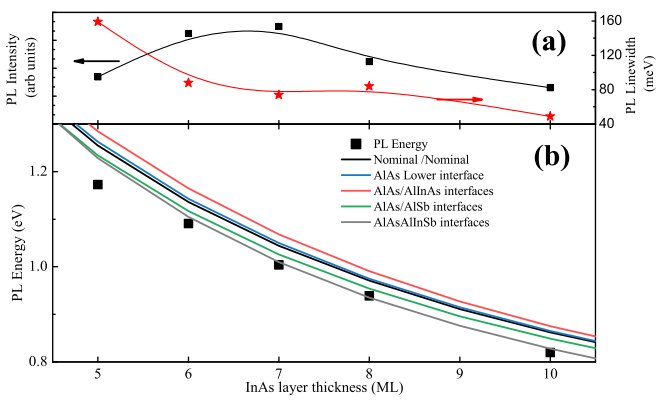

FIG. 4. Low temperature (20 K) experimental PL measurements for 5 to 10 ML thick InAs/AlAsSb QWs, (a) PL peak intensity and PL linewidth versus thickness and (b) PL energy as function of InAs nominal thickness: experimental data (squares), k·p calculations with the nominal band gap structure (black line) and including various interfacial layers (color lines) For each calculated curve, the composition of the lower/upper interfaces is indicated. The width of interfaces was set at 1 ML.

First, a 1ML strained AlAs layer was inserted at InAs on AlAsSb interface. It results in a weak change of transition energy. Therefore, the formation of arsenic rich AlAsSb layer deduced from HREM analysis cannot itself explain the observed shifts with experiments. In the following, we keep this layer at InAs on AlAsSb interface. The phenomena at the other interface are more complex. In a first attempt to describe this interface, we consider In to Al exchange and indium segregation into AlAsSb barriers. The insertion of AlInAs layers results of weak increase of transition energy. It is mainly due to the QW thinning induce by Indium segregation. Next, we consider the incorporation in $AlAs_{0.56}Sb_{0.44}$ barrier of the large amounts of Sb atoms supplied on the growth front during the deposition of InAs. In addition with indium segregation, this phenomenon leads to the formation of Sb rich AlInAsSb alloys at interface. The calculations for various AlInAsSb interfacial layer compositions show a large decrease of transition energies (Fig. 4(b)). The best fit is obtained for upper AlInSb interface though care must be taken since band structure and offset parameters of these highly strained layers is not accurately known. Note that it is consistent with local strain measurement and well reported antimony segregation.

To summarize InAs/AlAsSb QWs are promising for ISBT applications operating in 1.55 μm band. An interesting feature of Sb mediated growth is its ability to maintain a 2D growth mode over a thickness more than two times larger

than for conventional growth. Up to 7 ML thick strained InAs QWs were grown with no sign of plastic relaxation as shown by X ray diffraction and TEM. This opens up alternative ways to reach and use ISBT in the telecom range on this material system. Complementary HREM and Geometric Phase Analysis show gradual interface at nanoscale. The InAs-on-AlAsSb interface is under tensile strain, which is attributed to Sb-depletion in the topmost layers of lower AlAsSb barrier. On the contrary, the AlAsSb-on-InAs interface shows high-level of compressive strain. By modelling various QWs profiles, we conclude that In-segregation and incorporation of Sb atoms supplied during the surfactant mediated growth of InAs are together responsible for difference between experimental and theoretical transition energies.

This work was supported by the French National Research Agency (ANR) thought the project NAIADE. Yu Zhao would like to thank China Scholarship Council for financial support.

[1]R. Rapaport, G. Chen, O. Mitrofanov, C. Gmachl, H. M. Ng, and S. N. G. Chu, Appl. Phys. Lett. **83**, 263 (2003).
[2]T. Ogasawara, S. Gozu, T. Mozume, K. Akita, R. Akimoto, H. Kuwatsuka, T. Hasama, and H. Ishikawa, Appl. Phys. Lett. **98**, 251104 (2011).
[3]O. Lecrec, B. Lavigne, D. Chiaroni, and E. Desurvire, *Optical Fiber Communications IV A* (Academic, San Diego, 2002).
[4]J. D. Heber, C. Gmachl, H. M. Ng, and A. Y. Cho, Appl. Phys. Lett. **81**, 1237 (2002).
[5]M. Tchernycheva, L. Nevou, L. Doyennette, F. H. Julien, E. Warde, F. Guillot, E. Monroy, E. Bellet-Amalric, T. Remmele, and M. Albrecht, Phys. Rev. B **73**, 125347 (2006).
[6]B. S. Li, R. Akimoto, K. Akita, and T. Hasama, Appl. Phys. Lett. **88**, 221915 (2006).
[7]C. V.-B. Tribuzy, S. Ohser, S. Winnerl, J. Grenzer, H. Schneider, M. Helm, J. Neuhaus, T. Dekorsy, K. Biermann, and H. Künzel, Appl. Phys. Lett. **89**, 171104 (2006).
[8]P. Cristea, Y. Fedoryshyn, and H. Jäckel, "Growth of AlAsSb/InGaAs MBE-layers for all-optical switches," J. Cryst. Growth **278**, 544 (2005).
[9]T. Mozume, H. Yoshida, A. Neogi, and M. Kudo, Jpn. J. Appl. Phys., Part 1 **38**, 1286 (1999).
[10]J. Kasai and T. Mozume, J. Cryst. Growth **278**, 183 (2005).
[11]P. Cristea, Y. Fedoryshyn, J. F. Holzman, F. Robin, H. Jäckel, E. Müller, and J. Faist, J. Appl. Phys. **100**, 116104 (2006).
[12]H. Li, J. Wu, B. Xu, J. Liang, and Z. Wang, Appl. Phys. Lett. **72**, 2123 (1998).
[13]A. Ponchet, A. Le Corre, H. L'Haridon, B. Lambert, and S. Salaün, Appl. Phys. Lett. **67**, 1850 (1995).
[14]C. Gatel, H. Tang, C. Crestou, A. Ponchet, N. Bertru, F. Doré, and H. Folliot, Acta Mater. **58**, 3238 (2010).
[15]L. Tapfer and K. Ploog, Phys. Rev. B **40**, 9802 (1989).
[16]A. Mazuelas, L. Gonzalez, F. A. Ponce, L. Tapfer, and F. Briones, J. Cryst. Growth **131**, 465 (1993).
[17]J. M. Jancu, R. Scholz, F. Beltram, and F. Bassani, Phys. Rev. B **57**, 6493 (1998).
[18]M. J. Hytch, E. Snoeck, and R. Kilaas, Ultramicroscopy **74**, 131 (1998).
[19]V. Swaminathan, *Materials Aspects of GaAs and InP Based Structures* (Prentice-Hall, Inc., 1991).
[20]Q. Wang, Z. L. Wang, T. Brown, A. Brown, and G. May, J. Cryst. Growth **242**, 5 (2002).
[21]X. Wallart, S. Godey, Y. Douvry, and L. Desplanque, Appl. Phys. Lett. **93**, 123119 (2008).
[22]R. Kaspi and K. R. Evans, J. Cryst. Growth **175–176**(Pt. 2), 838 (1997).
[23]M. Pristovek, M. Zorn, U. Zeimer, and M. Weyers, J. Cryst. Growth **276**, 347 (2005).
[24]V. Haxha, I. Drouzas, J. M. Ulloa, M. Bozkurt, P. M. Koenraad, D. J. Mowbray, H. Y. Liu, M. J. Steer, M. Hopkinson, and M. A. Migliorato, Phys. Rev. B **80**, 165334 (2009).
[25]I. Vurgaftman, J. R. Meyer, and L. R. Ram-Mohan, J. Appl. Phys. **89**, 5815 (2001).